Separation Science and Technology
Publication details, including instructions for authors and subscription information:
http://www.informaworld.com/smpp/title~content=t713708471

Gold(III) Recovery From HCl Solutions using Amberlite XAD-7 Impregnated with an Ionic Liquid (Cyphos IL-101)

R. Navarro[a]; I. Saucedo[a]; M. A. Lira[a]; E. Guibal[b]
[a] Universidad de Guanajuato, División de Ciencias Naturales y Exactas, Departamento de Química, Cerro de le Venada s/n Pueblito de Rocha, Guanajuato, Gto, Mexico [b] Ecole des Mines Alès, Laboratoire Génie de l'Environnement Industriel, Equipe BioPhysicoChimie des Interfaces, Alès cedex, France

Online publication date: 30 August 2010

To cite this Article Navarro, R. , Saucedo, I. , Lira, M. A. and Guibal, E.(2010) 'Gold(III) Recovery From HCl Solutions using Amberlite XAD-7 Impregnated with an Ionic Liquid (Cyphos IL-101)', Separation Science and Technology, 45: 12, 1950 — 1962
To link to this Article: DOI: 10.1080/01496395.2010.493116
URL: http://dx.doi.org/10.1080/01496395.2010.493116

Separation Science and Technology, 45: 1950–1962, 2010

ISSN: 0149-6395 print/1520-5754 online
DOI: 10.1080/01496395.2010.493116

Taylor & Francis
Taylor & Francis Group

Gold(III) Recovery From HCl Solutions using Amberlite XAD-7 Impregnated with an Ionic Liquid (Cyphos IL-101)

R. Navarro,[1] I. Saucedo,[1] M. A. Lira,[1] and E. Guibal[2]

[1]*Universidad de Guanajuato, División de Ciencias Naturales y Exactas, Departamento de Química, Cerro de le Venada s/n Pueblito de Rocha, Guanajuato, Gto, Mexico*

[2]*Ecole des Mines Alès, Laboratoire Génie de l'Environnement Industriel, Equipe BioPhysicoChimie des Interfaces, Alès cedex, France*

An ionic liquid (IL) (Cyphos IL-101) was immobilized on Amberlite XAD-7 using the dry impregnation method. Raw resin and extractant impregnated resins (EIR) were tested for Au(III) recovery from HCl solutions. Impregnating the resin increased sorption capacity. Au(III) was extracted by an ion exchange mechanism involving the binding of its chloro-complex ($AuCl_4^-$) to IL phosphonium cation. Sorption isotherms were very favorable with capacities up to 160 mg Au g^{-1} EIR in 0.01 M HCl solution. Intraparticle diffusion controlled uptake kinetics. Au(III) was efficiently desorbed using thiourea (in HCl solutions). The EIR could be recycled maintaining high efficiencies for sorption and desorption for at least five cycles.

Keywords Cyphos IL-101; diffusion; gold; isotherms; sorption extractant impregnated resin; uptake kinetics

INTRODUCTION

Precious and strategic metals, including platinum group metals (PGMs), gold and silver, are subject to strong variations of their prices. The strong demand, the refuge value they represent in crisis periods may explain this variation. In addition to conventional mining resources, more and more studies are dealing with the recovery of these metals from secondary sources, including waste materials. For example, discarded electronic devices, and computer waste materials can constitute valuable resources of PGMs. A series of separation processes (gravimetric, ferrous/nonferrous) are applied before entering into a hydrometallurgy path. Contrary to mining sources, which are processed by cyanide process, waste materials are frequently subjected to acidic treatments (1). Acidic leaching using hydrochloric acid or nitric acid leads to the production of effluents containing gold and a number of precious and base metals at low concentrations; there is a need for developing alternative processes to conventional processes such as resins (2–8), biosorbents (9–15), membrane processes (16–18), or solvent extraction (19–26). These processes have limitations regarding their efficiency or competitiveness for the recovery of metals ions from highly acidic solutions (biosorption) or low metal concentration ranges (membrane or solvent extraction processes) or for their environmental impact (loss of solvent and extractants, for example). Solvent extraction combined with resin (SIR, solvent impregnated resin, or EIR, extractant impregnated resins) allows limiting the release of extractant by confinement of the extractant in a porous support and allows high extraction efficiency to be reached. For example, gold recovery from chloride solutions was studied using Amberlite XAD-2 resin impregnated with a series of extractants, such as triisobutyl phosphine sulfide (Cyanex 471) (27,28), or trioctylmethylammonium chloride (29). In addition to conventional extractants, a new class of compounds has been recently tested for metal and organic compounds recovery: ionic liquids (ILs) can be used as extractants (30,31), or solvents for conventional extractant (32). Among these ionic liquids, tetraalkylphosphonium ILs have recently received great attention for the extraction of metal ions (33,34) or organic compounds (35,36). Though based on the same principle as conventional EIRs, the immobilization of an ionic liquid instead of the usual extractants opens the way for developing alternative materials with improved safety (less volatile, nonflammable, and nontoxic), high extraction efficiency in acidic solutions (high sorption capacities based on a more favorable stoichiometric ratio between the metal and the reactive groups) and selectivity (only the metals forming stable anionic complexes could be extracted). This is also a complementary work to other studies using similar IL immobilized in biopolymer capsules. The immobilization of the IL in a porous resin brings different mass transfer properties than in the case of the physical encapsulation in a polymer matrix.

Received 18 February 2010; accepted 31 March 2010.

Address correspondence to R. Navarro, Universidad de Guanajuato, División de Ciencias Naturales y Exactas, Departamento de Química, Cerro de le Venada s/n Pueblito de Rocha, Guanajuato, Gto., Mexico. Tel. & Fax: +52-473-7327468; E-mail: navarrm@quijote.ugto.mx

These ionic liquids can be also immobilized in biopolymer capsules (37–42) or impregnated on conventional resins (43) to prepare new EIR systems (44). These new EIR based on the immobilization of Cyphos IL-101 (tetraalkylphosphonium chloride) in alginate/gelatin capsules have been tested for the sorption of Pt(IV) (38), Pd(II) (37), Hg(II) (39), Au(III) (40), and Bi(III) (41) from HCl solutions. More recently, the immobilization of different types of Cyphos IL in the same kind of matrix has been investigated for Cd(II) recovery from HCl solutions (45). Gallardo et al. (43) investigated the immobilization of Cyphos IL-101 on Amberlite XAD-7 for the sorption of Zn(II) from HCl solutions. The same material is tested in this study for Au(III) recovery. The influence of HCl concentration on Au(III) sorption is evaluated for different IL loadings. In a second step, the sorption isotherms in (0.01 M HCl solutions) are obtained with different EIRs (loaded with increasing amounts of IL) in order to determine the stoichiometric ratio between IL and Au(III), and at different temperatures to evaluate the thermodynamics of the sorption process. In a third step, uptake kinetics studies are carried out varying IL loading, metal concentration, and temperature. The last part of the paper briefly discusses metal desorption and resin recycling.

MATERIALS AND METHODS

Materials

Amberlite XAD-7 was supplied by Sigma-Aldrich (Saint-Louis, U.S.A.). This is a polyacrylic acid ester type resin ([CH_2−CH(COOR)]n). The physical characteristics of the resin are summarized in Table 1 (43). Amberlite XAD-7 can be considered as a nonionic, moderately hydrophilic macroporous polymer. The resin was conditioned by the supplier with NaCl and Na_2CO_3 to retard bacterial growth. It was necessary cleaning it to remove salts and monomeric material present on the resin. The resin was therefore put into contact with ketone for 24 h at 25°C. After filtration under vacuum to remove excess ketone, the resin was rinsed with de-mineralized water. It was then washed with nitric acid (0.1 M) for 24 h. The resin was filtered under vacuum and then rinsed with de-mineralized water to a constant pH. Finally, it was put into contact with ketone for 12 h before being filtered under vacuum and dried in a roto-vapor at 80°C. Cyphos IL-101 was kindly supplied by Cytec (Canada). This is a phosphonium salt (tetradecyl(trihexyl)phosphonium chloride, C.A.S. number: 258864-54-9, formula weight: 519 g mol^{-1}). It is a slightly viscous room temperature ionic liquid. It is less dense than water and colorless to pale yellow. It is immiscible with water although it is sparingly soluble in water and can dissolve up to 8% water. The chemical structure is $[R_3R'P]^+$ Cl^-, where R = hexyl and R′ = tetradecyl. Other reagents (salts, acids...) were analytical grade and supplied by KEM (Mexico). Standard metal solutions were supplied by Perkin Elmer (U.S.A.).

TABLE 1
Physical properties of Amberlite XAD-7

Physical property	Value
Superficial area	450 m^2 g^{-1}
Particle size	20/60 mesh–250/850 μm
Resin porosity	0.55
Pore size (mean value)	85–90 Å
Pore volume	0.97–1.14 cm^3 g^{-1}
Skeletal density	1.24 g cm^{-3}

Resin Impregnation

In the present work, the extractant was immobilized on the resin by a physical technique. Different processes may be used for the physical impregnation of the resin including

(i) the wet method,
(ii) the dry method,
(iii) the impregnation in the presence of a modifying agent, or
(iv) the dynamic method (46).

Previous studies have shown that the dry method increases the stability of the extractant on the resin. The dry impregnation of the resin was actually performed by contacting 5 g of conditioned Amberlite XAD-7 with 25 mL of ketone for 24 h (47). Varying amounts of Cyphos IL-101, diluted in ketone, were added to the resin slurry for 24 h, under agitation. The solvent was then slowly removed by evaporation in a roto-vapor. The amount of extractant immobilized on the resin ($q_{Cyphos\ IL\text{-}101}$) was quantified by the following procedure. A known amount of impregnated resin (250 mg) was mixed with methanol (5 mL) for 24 h to dissolve the extractant, and the solvent was separated from the resin by decantation. The washing treatment was repeated four times. Finally, the resin was dried at 50°C for 24 h for final evaporation of the solvent. The mass difference ($M_{Cyphos\ IL\text{-}101}$) between impregnated ($M_{XAD\text{-}7/Cyphos\ IL\text{-}101}$) and the washed resin ($M_{XAD\text{-}7}$) was used to calculate the amount of the extractant immobilized on the EIR:

$$q_{CyphosIL\text{-}101} = \frac{M_{XAD\text{-}7/CyphosIL\text{-}101} - M_{XAD\text{-}7}}{M_{XAD\text{-}7/CyphosIL\text{-}101}} \quad (1)$$

The experimental procedure allowed the preparation of EIR containing from 57 mg extractant g^{-1} EIR up to 573 mg extractant g^{-1} EIR.

Sorption Procedures

Au(III) solutions were prepared in HCl solutions of different concentrations (0.01–8 M) with metal concentrations ranging between 20 and 550 mg Au L^{-1}. The sorption

experiments at equilibrium were performed by mixing the resin with Au(III) solutions for 24 h with a sorbent dosage (SD, solid/liquid ratio) fixed to $m/V = 2\,g\,L^{-1}$ (m: mass of sorbent, V: volume of solution). Preliminary kinetic experiments showed that the equilibrium was reached within less than 24 hours of contact. The contact was made on a reciprocal shaker (Cole Parmer 51502) with an agitation speed (v) of 150 movements per minute at constant temperature. After filtration the samples were analyzed by atomic absorption spectrometry (AAS Perkin Elmer AAnalyst 200). The amount of metal adsorbed (q, mg Au g^{-1} EIR, or mmol Au g^{-1} EIR) was calculated by the mass balance equation: $q = V(C_0 - C_{eq})/m$, where C_0 and C_{eq} (mg Au L^{-1}, or mmol Au L^{-1}) are the initial and equilibrium Au(III) concentrations, respectively. Uptake kinetics were performed by contact under agitation of a fixed amount of EIR (20 mg of resin loaded in the range 113–398 mg extractant g^{-1} EIR) with a fixed volume (50 mL; m/V: $0.4\,g\,L^{-1}$) of 0.01 M HCl solution containing varying concentrations (in the range 20–60 mg Au(III) L^{-1}). The sorption took place in a closed jacketed tank reactor under mechanical agitation. The spaces available around the axis of the stirrer and for sampling were small enough to prevent water evaporation and temperature variation. Temperature (T) was varied in the range 10–40°C. The samples were collected at fixed times by a syringe connected to a filtration grid and residual gold concentrations were determined by UV-Vis spectrometry at 305 nm (Varian Cary 50 Probe UV-Vis Spectrophotometer). After analysis, the samples were returned to the reactor in order to avoid variation in solution volume.

Desorption and Recycling Procedures

For the study of Au(III) desorption, 20 mg of EIR (extractant loading: 398 mg extractant g^{-1} EIR) was mixed with 10 mL of Au(III) solution (250 mg Au(III) L^{-1} in 0.01 M HCl solution) for 24 h. The residual concentration measured by AAS after filtration served to determine the amount of metal bound to the resin. The metal-loaded resin was mixed for 24 h with 10 mL of 1.0 M thiourea (in 0.1 M HCl). After filtration, the concentration in the eluent was determined by AAS in order to obtain the amount of Au desorbed from the resin. The amount of metal desorbed divided by the amount of metal bound to the EIR served for calculating the desorption yield (or efficiency).

For the evaluation of sorption/desorption cycles, the same procedure was used for five cycles. After the desorption step and before the sorption step, the resin was washed three times with 0.01 M HCl for 8 h in order to eliminate residual thiourea retained in the resin.

SEM and SEM-EDAX Analyses

Scanning electron microscopy (SEM) and SEM-EDAX (SEM coupled with energy dispersive X-ray analysis) were performed using an Environmental Scanning Electron Microscopy (ESEM) Quanta FEG 200, equipped with an OXFORD Inca 350 Energy Dispersive X-ray microanalysis (EDAX) system. The system can be used to acquire qualitative or quantitative spot analyses and qualitative or quantitative X-ray elemental maps and line scans. This ESEM allows samples to be analyzed at pressures and humidity which approach normal laboratory conditions and avoids experimental artifact. More specifically, this is possible to analyze the samples at much higher pressures than with conventional SEM. For cross-section analysis, the resin particles were frozen in liquid nitrogen prior to mechanical breaking in order to obtain observable cross-sections. This procedure prevents the section from becoming contaminated by element dispersion that can occur when the particles are embedded in a synthetic resin and cut as a thin slice with a microtome.

RESULTS AND DISCUSSION

EIR Characterization by SEM and SEM-EDAX Analyses

The EIR were cryo-fractured in order to analyze by SEM-EDAX the distribution of elements in the particles before and after metal sorption (Fig. 1). The distribution of the P element serves as a tracer for Cyphos IL-101 dispersion in the resin: the cartography of P element confirmed that the IL was homogeneously distributed in the whole mass of the resin (the distribution of the element along the cross-section is not shown but the intensity of the signal was constant along the axis) (Fig. 1(a)). The impregnation method allows diffusing and immobilizing the IL even in the center of the particle (no concentration gradient). After metal sorption, the cartography of the P element did not change. The distributions for Cl and Au elements were less homogeneous: at the center of the particle the density for Cl was slightly reduced, while a much denser concentration of Au was observed there. Though the impact of a dense element such as Au may impact the analysis of Cl element, this could indicate that a specific mechanism occurred at the center of the particle. Figure 1(b) shows the distribution of Au through the section and the SEM analysis (with retro-diffused electrons) of the center part with a much higher growing magnitude. The SEM view shows very dense agglomeration at the center of the resin particle, with the agglomeration size approaching 15 μm, and surrounded by the distribution of a number of smaller agglomerates (sub-micron dots). Gold is homogeneously distributed outside this central zone, associated with the phosphorous element on the phosphonium group, with nanosize scale. The difference in the order of magnitude and aspect, evidenced by the SEM analysis, suggests that a nucleation mechanism may be taking place, leading to the formation of micro-size aggregates. However, complementary experiments are

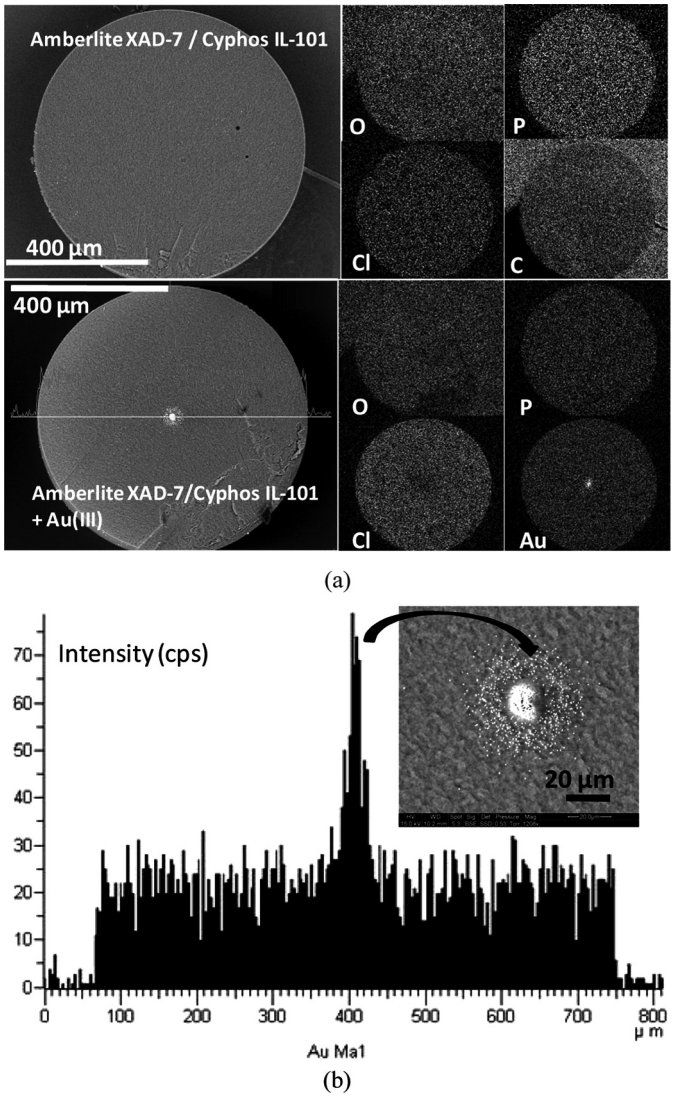

FIG. 1. SEM-EDAX analysis of Amberlite XAD-7/Cyphos IL-101 EIR before and after Au(III) sorption (IL loading 398 mg IL g^{-1}) (a: Element cartography; b: Au distribution along the cross-section and retro-diffused electron view of the central part of the resin, i.e., gold aggregates).

required to confirm this hypothesis (checking the reproducibility and the effect of an oversaturation of the resin, mixing the loaded resin with fresh gold solutions for several cycles, for example).

Influence of HCl Concentration and IL Loading

The first study focused on the investigation of the impact of HCl concentration (0.01–8 M) and IL loading (57–573 mg IL g^{-1}) on Au(III) removal at equilibrium under selected experimental conditions. Figure 2 reports the evolution of the sorption efficiency (ratio of the amount of metal removed to the amount of metal initially present) with varying experimental parameters. The figure also reports Au(III) sorption efficiency on raw Amberlite XAD-7 resin. The raw resin showed appreciable sorption efficiency for Au(III): about 22% at 0.01 M HCl concentration, increasing to about 45% at 2 M HCl concentration. Above 2 M HCl concentration, the efficiency remained stable.

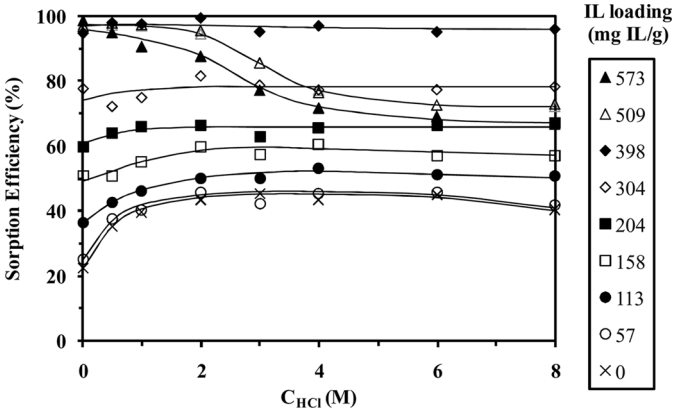

FIG. 2. Influence of HCl concentration and IL loading on Au(III) sorption efficiency using Amberlite XAD-7/Cyphos IL-101 (Sorbent dosage, SD: 2 g L^{-1}; v: 150 rpm; T: 20°C; Agitation time: 24 h; C_0: 300 mg Au L^{-1}).

Villaescusa et al. (28) investigated Au(III) binding in HCl solutions using a resin bearing polyacrylic acid ester functions ($[CH_2-CH(COOR)-]_n$). Based on their findings, they suggested that highly acidic solutions induced the hydrolysis of polyacrylic acid ester functions that were converted into RCOOH functions. These carboxylic acid groups, in turn, bound Au(III) through the binding of an ion pair ($HAuCl_4$). More recently, Navarro et al. (48) observed that polyamide membranes ($[R-NH-(C=O)R]_n$), after being immersed into acidic solutions, have been chemically modified (partial hydrolysis of amide groups). They retain mineral acids in the polymer membrane through interactions such as $=O \cdot\cdot H^+X^-$.

In the case of XAD-7 resin, similar behavior can be expected; HCl is extracted by the resin through interaction with oxygen of polyacrylic matrix ($=O \cdot\cdot H^+Cl^-$). Chloride ions can be exchanged with the anionic complex according: $= O \cdot\cdot H^+MCl_4^-$. In the same way, the sorption of a series of trivalent metals, including Fe(III) on Amberlite XAD-7 resins in highly acidic solutions has been reported. These studies concluded that the metals were adsorbed by the interaction between protonated oxygen atoms of polyacrylate and chloro-complexes to form $= O \cdot\cdot H^+MCl_4^-$ (49,50).

Similar reactions have been proposed by Laatikainen and Paatero (51) for the Au(III) extraction on Amberlite XAD-7 in HCl solution. They proposed two mechanisms for the binding of gold chloro-complexes on the resin:

(i) first the protonation of carbonyl groups by HCl, followed by the exchange with tetrachloroauric acid; or alternatively
(ii) hydrophobic interactions with adsorbable complexes of low charge.

However, they conclude that the protonation mechanism (also observed in mild acidic conditions) is not sufficient to explain the high sorption levels obtained in their study. They concluded that hydrophobic interactions may be more likely to justify the high levels on gold sorption they observed. Similar hydrophobic interactions have been proposed in the extraction of $FeCl_4^-$, preferentially to other Fe(III) species. The tetrachloroferrate anion has a tetrahedral structure and it does not contain water ligands and thus is the most hydrophobic of the Fe(III) chloro-complexes. The hydrophobicity and the absence of a dipole moment have been proposed as crucial factors in the distribution of the complex between aqueous and organic phases (51).

The interaction of HCl with carboxylic groups on the resin can be described by the following reaction:

$$R + H^+ + Cl^- \leftrightarrows RHCl \quad (2)$$

here R and RHCl represent the resin under the neutral form and loaded with HCl, respectively. The predominant form of the resin depends on HCl concentration in the solution. The conversion of R into RHCl takes place when HCl concentrations reaches 7–8 M (50). Gold speciation reported by Baes and Mesmer (52) showed that $AuCl_4^-$ remains the predominant species, regardless of HCl concentration (under our experimental conditions). The extraction reaction could be described by Eqs. (3) and (4), depending on the predominant form of the resin, which is controlled by HCl concentration:

$$AuCl_4^- + R + H^+ \leftrightarrows RHAuCl_4 \quad (3)$$

$$AuCl_4^- + RHCl \leftrightarrows RHAuCl_4 + Cl^- \quad (4)$$

Equation (3) appears more appropriate for describing the increase in the efficiency of gold extraction with the increase of HCl concentration, shown on Fig. 2. However, at high HCl concentration (8 M), Eq. (4) explains the small decrease of extraction efficiency due to the competition of anion Cl^- at high concentration. A significant decrease of metal extraction efficiency was also reported for Fe(III) extraction by Amberlite XAD-7 at high HCl concentration (>7 M) (50). When increasing IL loading, different behaviors were observed, depending on the degree of saturation of the resin. At low IL loading (i.e., 57 mg IL g^{-1}), the sorption efficiency was almost superimposed to the curve obtained with raw Amberlite XAD-7. In the range 113–398 mg IL g^{-1}, sorption efficiency increased with IL loading. These first data suggest that a part of the IL probably interacted with the support, losing its ability to gold binding. A similar phenomenon was observed in the case of Cd(II) sorption using the same EIR (Cyphos IL-101/Amberlite XAD-7 in HCl solutions) (53).

Gold recovery proceeds through a combination of extraction processes including sorption on the polymer matrix and extraction by the IL. Gold removal from HCl solutions has also been investigated using Cyphos IL-101 immobilized in a composite alginate/gelatin biopolymer matrix (40). Gold binds through the interaction of $R_3R'P^+$ with $AuCl_4^-$ by an ion exchange mechanism between gold chloro-anionic species and chloride ions bound to the IL. The extraction process can be described by the reaction:

$$AuCl_4^- + L^+Cl^- \leftrightarrows L^+AuCl_4^- + Cl^- \quad (5)$$

where L^+Cl^- is the Cyphos IL-101 impregnated in the resin (L^+: tetraalkylphosphonium), and $L^+AuCl_4^-$ is the gold species adsorbed in the EIR.

With low IL loadings (i.e., 113–398 mg IL g^{-1}), increasing HCl concentration up to 2 M slightly increased sorption efficiency; above 2 M concentration the sorption efficiency tended to level off. This trend clearly appears for the lowest IL loadings and this can be explained by the combination of reactions 3–5. In the case of gold liquid/liquid extraction, using Cyphos IL-101, Campos et al. (40) showed that HCl concentration (in the range 0.1–5 M) did not influence the extraction efficiency. Regel-Rosocka's group investigated the liquid/liquid extraction of Zn(II) and Pd(II) chloro-anions (33,34) using Cyphos ionic liquids. Ciezynska et al. (33) observed the influence of Pd(II) speciation on metal extraction. Species such as $PdCl_4^{2-}$ and $PdCl_3^-$ were extracted at high (above 3 M) and low (about 0.1 M) HCl concentration, respectively. This changed the stoichiometric ratio between the ligand and the metal species (from 2:1 to 1:1, respectively). With Cyphos IL-101 immobilized in biopolymer matrices, the concentration of HCl weakly affected the sorption of Pd(II) (37) and Au(III) (40). For metals such as Hg(II) (39), Pt(IV) (38), and Bi(III) (41) the impact was almost not detectable since their speciation is almost independent of HCl concentration. For Zn(II) sorption on Cyphos IL-101/Amberlite XAD-7, Gallardo et al. (43) observed that $ZnCl_4^{2-}$ was bound to the EIR, regardless of the HCl concentration. However, the number of exchanged chloride ions varied with HCl concentration and metal speciation. At low HCl concentration $ZnCl_3^-$ predominates in aqueous solution and metal sorption proceeds by the exchange of one Cl^-. At high concentration the predominance of $ZnCl_4^{2-}$ induced the exchange of two Cl^-.

Under selected experimental conditions, maximum Au(III) recovery was obtained at intermediary IL loading (i.e., 398 mg IL g^{-1}) and with sorption efficiency maintained above 94%. For higher IL loadings (i.e., >500 mg IL g^{-1}) the sorption efficiency decreased (down to 70%), especially at high HCl concentration (i.e., >3 M). Gallardo et al. (43) did not observe similar trends

in the case of Zn(II) extraction using the same EIR. It is difficult to explain these differences in the extraction behavior. Though no proof is available at this stage, it is suspected that this decrease in the sorption efficiency could be explained by the incapacity of the resin to stably immobilize large amounts of extractants, especially in very acidic conditions: at high IL loading; the excess of extractant is expulsed from the internal porous network. This simultaneously causes gold release from the resin. This effect is reinforced, at high HCl concentration, by the extraction of water and HCl; Avila-Rodriguez et al. (54) observed that Cyphos IL-101 can extract significant amounts of water and HCl, which increase with HCl concentration. This extraction causes, in turn, an increase of the volume of the extractant phase in the porous network: at high IL loading resin internal volume is not sufficient to maintain the organic phase, and the extractant phase is partially released. For these reasons, it appeared preferable limiting IL loading strictly below 500 mg IL g^{-1} (i.e., 100–400 mg IL g^{-1}). Complementary experiments are currently in progress for evaluating the amount of HCl in the pores of the resin. However, the information is quite difficult to obtain since HCl can be present both in the aqueous phase filling the porous network and in the IL phase. It is difficult to separate the respective contributions of these two HCl forms in the EIR.

Figure 3 shows Au(III) sorption capacity of the resins at different HCl concentrations as a function of IL loading (limiting the representation of data to IL loadings in the range 0–398 mg IL g^{-1}, due to the instability of EIR at higher IL loadings). The data can be separated in two groups: at low HCl concentration (below 1 M) the sorption capacities were substantially below the trends followed at higher HCl concentration (especially for IL loading below 150 mg IL g^{-1}). At HCl concentration higher than 1 M the differences were not so marked. For the group of data corresponding to HCl concentration greater (or equal) to 1 M and IL loading in the range 113–398 mg IL g^{-1} it was possible to linearly correlate sorption capacity to IL loading (grey continuous line on Fig. 3): ordinate intercept was close to 45 mg Au g^{-1}. And the slope of the curve was close to 0.23 mg Au/mg IL; this means a molar ratio 0.60 mol Au/mol IL. At low IL loading (i.e., 0–58 mg IL g^{-1}), and for HCl concentrations below 1 M, the sorption capacity remained constant and close to 59 mg Au g^{-1} (horizontal trend). The intersection of the two straight lines delimits a critical point corresponding to a sorption capacity close to 60 mg Au g^{-1} for an IL loading close to 63 mg IL g^{-1}. This limiting sorption capacity approximately corresponds to the sorption capacity of raw Amberlite XAD-7; the limit IL loading corresponds to the amount of IL that interacts with the support without reacting with metal ions. This corresponds more or less to the previous observation: at the IL loading of 57 mg IL g^{-1}, sorption capacity was not changed compared to raw resin. This part of the IL does not react with metal ions but does not limit the ability of Amberlite XAD-7 to bind Au(III) chloro-anions. The slope of the curve corresponds to a molar ratio 0.60 mol Au/mol IL (or 1.66 mol IL/mol Au). This molar ratio is significantly greater than the molar ratio expected for the 1:1 interaction between $AuCl_4^-$ and $R_3R'P^+$. This can probably be explained by the fact that the EIR was not fully saturated under selected experimental conditions.

Figure 4 shows the log-log plot of the distribution coefficient (defined as $D = q/C_{eq}$, L kg^{-1}) versus IL loading of the EIR, in the 0.01–8 M HCl concentration range. For IL loadings in the range 113–304 mg IL g^{-1}, the log D linearly correlated to log IL loading: the slope of the curve was

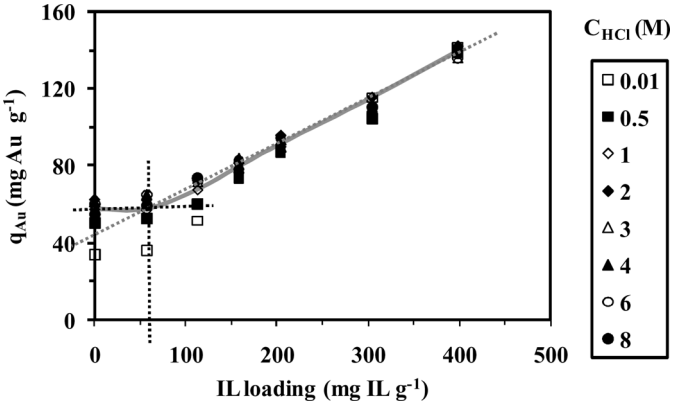

FIG. 3. Influence of HCl concentration and IL loading on Au(III) sorption capacity using Amberlite XAD-7/Cyphos IL-101 (SD: 2 g L^{-1}; v: 150 rpm; T: 20°C; Agitation time: 24 h; C_0: 300 mg Au L^{-1}; continuous grey line shows the average value for 1–8 M HCl concentration; dot lines show the identification of the limit point for resin internal coverage).

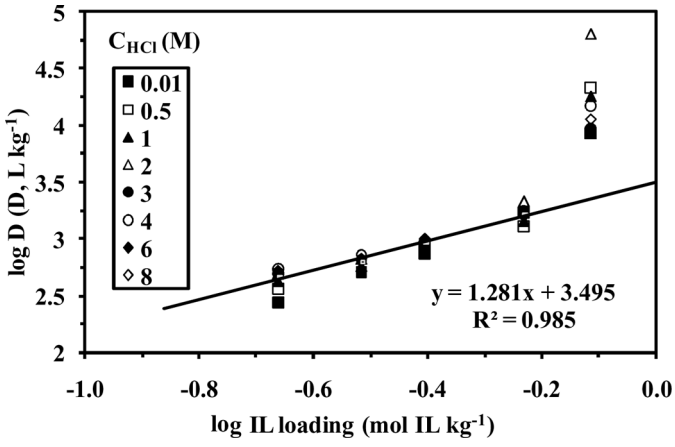

FIG. 4. Influence of IL loading and HCl concentration on the distribution coefficient of Au(III) (SD: 2 g L^{-1}; v: 150 rpm; T: 20°C; Agitation time: 24 h; C_0: 300 mg Au L^{-1}).

close to 1.28. This slope represents the molar ratio IL to Au (IL:Au) and is expected to be 1:1. Note that the value obtained from Fig. 4 (1.28) is closer to unity than that obtained from Fig. 3 (1.66). Surprisingly, for the 398 mg IL g^{-1} loading, the distribution coefficient sharply increased, leaving the linear trend: the dispersion of data (with HCl concentration) and the high values of D can probably be explained by the low residual concentrations of Au(III) with higher analytical uncertainty that caused significant variation in the distribution coefficient.

Sorption Isotherms

Sorption isotherms have been carried out in 0.01 M HCl solutions, testing the influence of IL loading (Fig. 5) and temperature (Fig. 6). Raw Amberlite XAD-7 (without immobilizing Cyphos IL-101) shows a maximum sorption capacity lower than 34 mg Au g^{-1}; additionally, the affinity of the resin for gold (represented by the initial slope of the curve) is quite low, compared to the profiles obtained

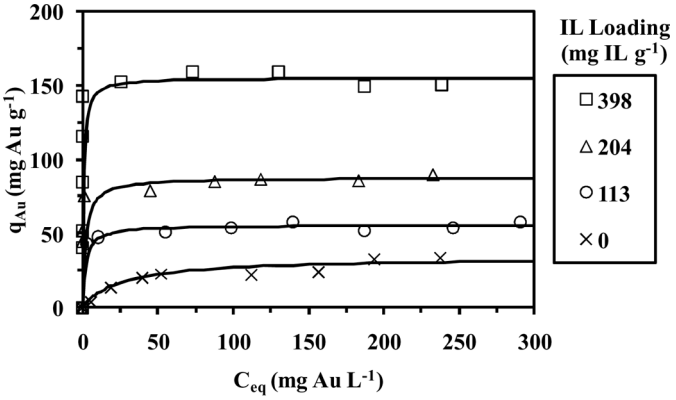

FIG. 5. Influence of IL loading on Au(III) sorption isotherms using EIR (a), and relationship between sorption capacity and IL loading (b) (SD: 2 g L^{-1}; v: 150 rpm; T: 20°C; Agitation time: 24 h; C_{HCl}: 0.01 M).

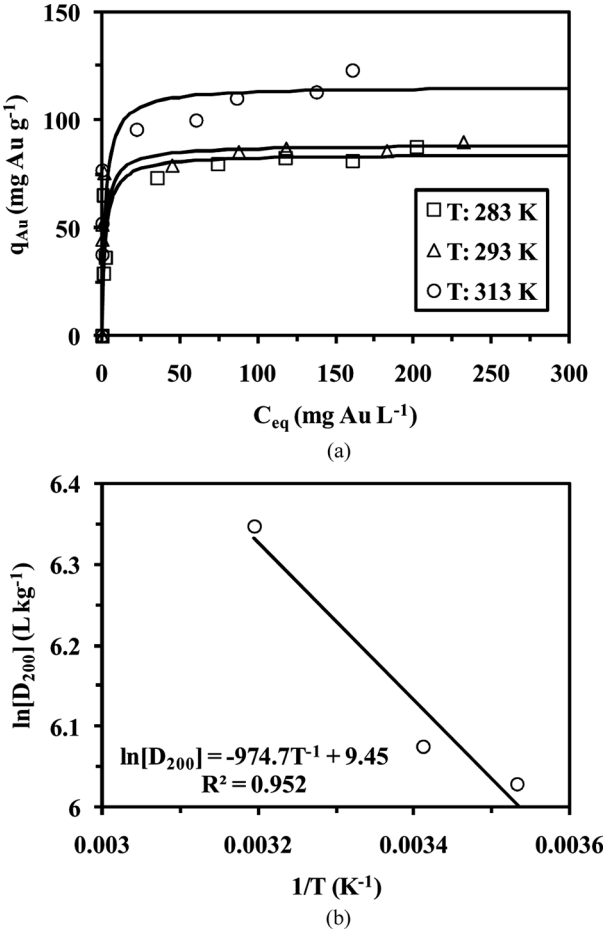

FIG. 6. Influence of temperature on Au(III) sorption isotherms (a), and thermodynamic data (b) (SD: 2 g L^{-1}; v: 150 rpm; Agitation time: 24 h; C_{HCl}: 0.01 M; IL loading: 204 mg IL g^{-1}).

with EIRs. Experimental data were modeled using the Langmuir equation:

$$q = \frac{q_m b C_{eq}}{1 + b C_{eq}} \quad (6)$$

where q, q_m (mg g^{-1}, or mmol g^{-1}) are sorption capacities in equilibrium with C_{eq} (mg L^{-1}, or m mol L^{-1}) and at saturation of the monolayer, respectively; b is the affinity coefficient (L mg^{-1}, or L $mmol^{-1}$). The shape of the sorption isotherms that form a saturation plateau at low residual concentration suggest that the Langmuir equation is more appropriate than the Freundlich equation (which assumes an exponential trend).

Influence of IL Loading

Figure 5(a) shows that EIR are characterized by very favorable sorption isotherms (sharp initial slope and saturation plateau reached at low residual concentration), that makes "delicate" the determination of the parameters of

TABLE 2
Coefficients of the Langmuir equation for Au(III) sorption isotherms using Cyphos IL-101/Amberlite XAD-7 EIR (Sorbent dosage, SD: 2 g L^{-1}; v: 150 rpm; Agitation time: 24 h; C_{HCl}: 0.01 M)

IL loading (mg IL g^{-1})	T (°C)	q_m (mg g^{-1})	b (L mg^{-1})	R^2	N(IL/Au) (mol/mol)
0	20	33.5	0.04	0.999	–
113	20	55.3	0.485	0.999	0.78
204	20	87.9	0.514	0.999	0.88
398	20	155.3	1.48	0.999	0.97
204	10	84.0	0.464	0.999	0.92
204	40	115.4	0.454	0.999	0.67

N is the molar ratio between the Cyphos IL 101 in the resin and gold at saturation of the EIR.

the model. Table 2 summarizes the parameters of the Langmuir equation that serves for plotting the simulated curves (continuous lines on Fig. 5(a)). Increasing IL loading increased the maximum sorption capacity. Figure 5(b) shows that the increase in sorption capacity can be linearly correlated to IL loading between 113 and 398 mg IL g^{-1}. The maximum sorption capacity for raw Amberlite XAD-7 resin does not correspond to the ordinate intercept of the curve (18 mg Au g^{-1} versus 33.5 mg Au g^{-1}), as another evidence of the dual sorption mode (raw resin + IL). Plotted in molar units, the maximum sorption capacity vs. IL loading shows a slope close to 0.92 mol Au/mol IL. This stoichiometric ratio is consistent with the 1:1 expected molar ratio between $AuCl_4^-$ and $R_3R'P^+$. For Zn(II) sorption using the same EIR, Gallardo et al. (43) obtained a stoichiometric ratio close to 0.5 for the interaction of $ZnCl_4^{2-}$ and $R_3R'P^+$. In the case of gold binding on Cyphos IL-101 immobilized in biopolymer capsules, Campos et al. (40) obtained sorption capacities close to 200 mg Au g^{-1} in 1 M HCl solutions, for the alginate capsules bearing the highest IL load. The stoichiometric ratio was found close to the theoretical stoichiometric ratio (1.02 ± 0.03 versus 1:1). The series of studies carried out by Guibal's group using Cyphos IL-101 immobilized in biopolymer capsules has correlated the stoichiometric ratio IL/Metal to the anionic charge of the target metal chloro-complex (37–41). The only significant variation against this theoretical IL/metal ratio was observed in the case of Pd(II) (37); for which the speciation changed in the 0.1–5 M HCl concentration range.

Influence of Temperature

In the case of Zn(II) sorption using the same EIR, Gallardo et al. (43) did not find significant differences in maximum sorption capacity and found negligible variations in the affinity coefficient with varying the temperature. This is slightly different in the present case: the sorption isotherm almost overlapped between 10 and 20°C (i.e., 283 K and 293 K), while a significant increase of sorption capacity was observed when the temperature rose to 40°C (i.e., 313 K). The affinity coefficient (i.e., b coefficient) hardly varied with temperature. The distribution coefficient ($D = q_{eq}/C_{eq}$, L kg^{-1}) was calculated for the three sorption isotherms using the Langmuir equation with model parameters summarized in Table 2 for a residual concentration of 200 mg Au L^{-1} (D_{200}, on the saturation plateau). The equilibrium constants were correlated to the reciprocal of temperature according the Van't Hoff equation [15,55]:

$$\ln D_{200} = \frac{-\Delta H^\circ}{RT} + \frac{\Delta S^\circ}{R} \tag{7}$$

where ΔH° is the change in enthalpy (kJ mol^{-1}), R is the universal gas constant (8.314 J mol^{-1} K^{-1}), T is the absolute temperature (K), and ΔS° is the entropy change (kJ mol^{-1} K^{-1}).

From Fig. 6(b) the change in enthalpy was found to be close to 8.1 kJ mol^{-1}, and the entropy change was 78.6 J mol^{-1} K^{-1}. The process is endothermic (ΔH° being positive). This is consistent with the endothermic nature of the sorption process as indicated by the increase of sorption capacity with temperature. The enthalpy change found in the present system is much lower than the values found by Martinez et al. (56) and Barroso et al. (57) for gold extraction by the solvation mechanism using Cyanex 921 and Cyanex 925, respectively (in liquid/liquid extraction). The positive value of ΔS° shows that the sorption of gold is correlated to an increased randomness. Shu et al. (58) investigated the thermodynamics of chlorobenzene sorption on CTMAB modified bentonite and kaolinite. They explain the positive value of entropy by the rearrangement of sorbate in a more chaotically distribution at the surface of the sorbent than in the solution. Guerra et al. (59) carried out uranyl sorption on modified attapulgite. They pointed out that uranyl ions should not be solvated for binding at the surface of the sorbent. During metal sorption, the solvated species are modified leading to the release of solvent molecules that promotes the disorganization of the system. The interaction of the metal with the ligand, the extraction of water and HCl in the IL phase may also contribute to increasing the entropy and disorder of the EIR system.

The Gibbs free energy (ΔG°, J mol^{-1}) was calculated from the Gibbs-Helmholtz equation:

$$\Delta G^\circ = \Delta H^\circ - T\Delta S^\circ \tag{8}$$

At room temperature, the Gibbs free energy was close to -14.9 kJ mol^{-1}; this means that the sorption process is

spontaneous. In the case of gold sorption using a lysine derivative of chitosan Fujiwara et al. (15) observed that the adsorption process was exothermic (ΔH° being negative) and spontaneous (ΔG° being negative).

Uptake Kinetics

Uptake kinetics may be controlled by several mechanisms including resistance to diffusion (film diffusion and/or intraparticle diffusion) and chemical reaction. The identification of the controlling step is important for optimizing the process; this allows selecting the best experimental conditions or optimizing the design of the sorbent (for limiting, for example, resistance to intraparticle diffusion). Actually, the modeling of uptake kinetics should take into account all these mechanisms (film diffusion, intraparticle diffusion, reaction rate, equilibrium distribution...) at the expense of using complex numerical analysis systems (60). Juang and Ju (61) discussed a series of simplified modeling systems derived from the homogeneous diffusion model (HDM) and the shrinking core model (SCM). The HDM involves counterdiffusion of exchangeable species in quasi homogeneous media, with a contribution from film diffusion (HDM-FD) and/or particle diffusion (HDM-PD). Solute molecules and exchangeable species (immobilized on the resin) follow a similar diffusion mechanism (but in the opposite direction). In the case of the SCM, a sharp virtual boundary exists between the reacted shell of the particle and the unreacted core, and this boundary moves towards the center of the particle (62,63). This model was developed with different systems depending on the controlling step: film diffusion (SCM-FD), particle diffusion (SCM-PD) and chemical reaction rate (SCM-CR) (61). A number of mathematical equations have been developed to simulate these mechanisms, they are listed below:

Homogeneous Diffusion Model

$$\text{Film Diffusion}: \quad F_1(X) = -\ln(1-X) = f(t) \tag{9}$$

$$\text{Particle Diffusion}: \quad F_2(X) = -\ln(1-X^2) = f(t) \tag{10}$$

Shrinking Core Model

$$\text{Film Diffusion}: G_1(X) = X = g\left(\int_0^t C(t)dt\right) \tag{11}$$

Particle Diffusion :

$$G_2(X) = 3 - 3(1-X)^{2/3} - 2X = g\left(\int_0^t C(t)dt\right) \tag{12}$$

Chemical Reaction Rate :

$$G_3(X) = 1 - (1-X)^{1/3} = g\left(\int_0^t C(t)dt\right) \tag{13}$$

Here X is the fractional approach to equilibrium (i.e., $q(t)/q_{eq}$), the amount adsorbed at time t divided by the amount of metal adsorbed at equilibrium. Plotting F_i and G_i functions versus time and the integral term (respectively) determined the most appropriate mechanism for describing the controlling step. The curve giving a straight line (good correlation measured by the correlation coefficient) is the predominant limiting step. Equations (9)–(13) have been tested for each experimental series, and the best fits of experimental data were systematically obtained with the equations making the intraparticle diffusion resistance the limiting step (not shown).

The intraparticle diffusion coefficient (D_e, effective diffusivity, $m^2\,min^{-1}$) was determined using Crank's equation, assuming the solid to be initially free of metal, and the kinetics to be controlled by intraparticle diffusion resistance (64):

$$\frac{q(t)}{q_{eq}} = 1 - \sum_{n=1}^{\infty} \frac{6\alpha(\alpha+1)\exp\left(\frac{-D_e q_n^2 t}{r^2}\right)}{9 + 9\alpha + q_n^2\alpha^2} \tag{14}$$

$q(t)$ and q_{eq} are the concentrations of the metal in the resin at time t and equilibrium, respectively.

And q_n are non-zero roots of the equation:

$$\tan q_n = \frac{3q_n}{3 + \alpha q_n^2} \tag{15}$$

with

$$\frac{q}{VC_o} = \frac{1}{1+\alpha} \tag{16}$$

The Mathematica™ software was used for the determination of the intraparticle diffusion coefficient, D_e, and for the simulation of experimental data (represented by the continuous line on Figs. 7–9). The intraparticle diffusion coefficients, D_e, were determined for each experimental series and the values are compiled in Table 3. The intraparticle diffusion coefficient varied between $1.8 \times 10^{-11}\,m^2\,min^{-1}$ and $17 \times 10^{-11}\,m^2\,min^{-1}$. These values are comparable to those cited by Campos et al. (40) for gold sorption using Cyphos IL-101 immobilized in biopolymer capsules (i.e., in the range 1×10^{-11}–$4 \times 10^{-11}\,m^2\,min^{-1}$) or those reported by Navarro et al. (50) for Fe(III) sorption using Cyanex 921 impregnated in XAD-7 resin (i.e., in the range 1×10^{-11}–$47 \times 10^{-11}\,m^2\,min^{-1}$).

Influence of IL Loading on Uptake Kinetics

IL loading affects the sorption capacity of the resin (according Fig. 5); however, this parameter may also

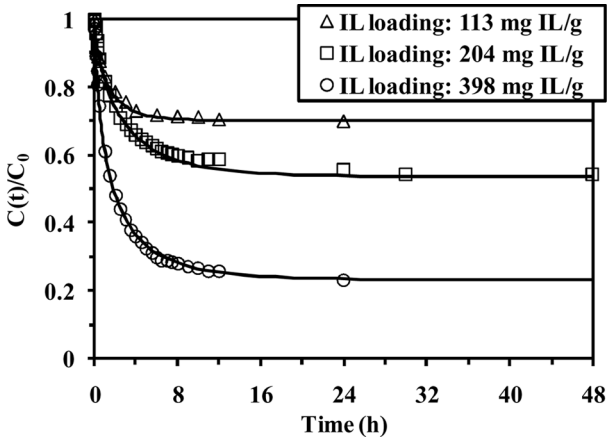

FIG. 7. Influence of IL loading on Au(III) sorption kinetics using EIR (SD: 0.4 g L^{-1}; v: 150 rpm; C_{HCl}: 0.01 M; T: 20°C; C_0: 53 mg Au L^{-1}).

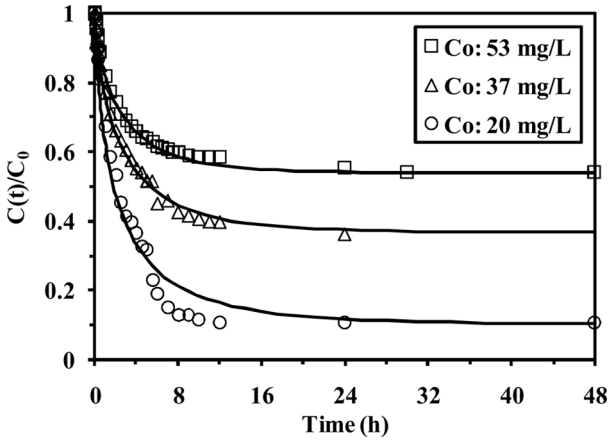

FIG. 8. Influence of Au(III) concentration on sorption kinetics using EIR (SD: 0.4 g L^{-1}; v: 150 rpm; C_{HCl}: 0.01 M; T: 20°C; IL loading: 204 mg IL g^{-1}).

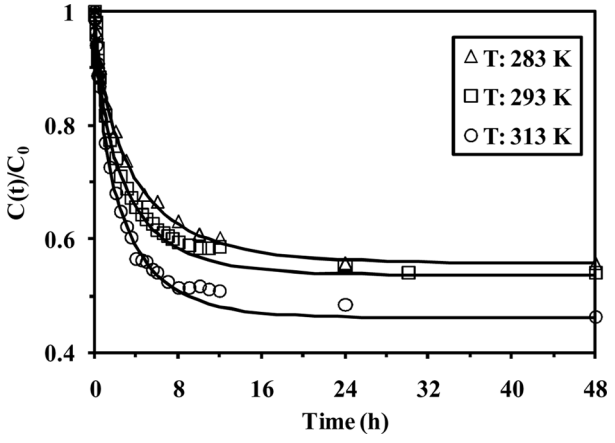

FIG. 9. Influence of temperature on Au(III) sorption kinetics using EIR (SD: 0.4 g L^{-1}; v: 150 rpm; C_{HCl}: 0.01 M; C_0: 53 mg Au L^{-1}; IL loading: 204 mg IL g^{-1}).

TABLE 3
Uptake kinetics for gold recovery from 0.01 M HCl solutions using Cyphos IL-101/Amberlite XAD-7 resin – Intraparticle diffusion coefficients (SD: 0.4 g L^{-1}; v: 150 rpm; Agitation time: 24 h; [HCl]: 0.01 M)

IL loading (mg IL g^{-1})	C_0 (mg Au L^{-1})	T (°C)	$D_e \times 10^{11}$ (m^2 min^{-1})	ERV
113	53	20	16.6	0.032
204	53	20	6.5	0.011
398	53	20	5.2	0.006
204	20	20	1.8	0.064
204	37	20	4.6	0.010
204	53	10	5.1	0.006
204	53	40	6.5	0.012

ERV: estimated error variance.

impact mass transfer. Indeed, as shown by Arias et al. (53), when increasing the loading of Amberlite XAD-7 with Cyphos IL-101 both the specific surface area of EIR and the adsorbed volume strongly reduced (while the size of pores increased). The loading of the porous network of the resin increased the mass transfer resistance to intraparticle diffusion for Cd(II) binding using the same system. Figure 7 shows that regardless of IL loading the equilibrium was reached within a comparable contact time (i.e., around 8 hours, under selected experimental conditions, for reaching up to 95% of total sorption). However, Table 3 demonstrates that the intraparticle diffusion coefficient tended to decrease (by a factor 3 when IL loading increased from 113 to 398 mg I L g^{-1}). As the IL loading increases, the porous network is progressively filled, and the mobility of the solute in the porous network of the resin decreases. For Au(III) sorption using Cyphos IL-101 immobilized in biopolymer capsules, Campos et al. (40) also commented that the intraparticle diffusion coefficient decreased with the amount of IL immobilized in the biopolymer network; however, the difference was less marked than in the present case. This difference is probably related to differences in the impact of internal porosity and IL immobilization: with Amberlite XAD-7 support the impregnation proceeded through immobilization in the internal porosity of the resin, while in the case of biopolymer immobilization the IL was entrapped in the polymer matrix with less interconnectivity between IL vesicles.

Influence of Metal Concentration on Uptake Kinetics

Metal concentration was varied; Figure 8 shows that the intraparticle diffusion model fitted well experimental data: the simulated curve overlapped the experimental data, at least for higher metal concentrations. Table 3 indicates that the intraparticle diffusion coefficient increased with metal concentration in the solution. A larger concentration in

the solution means a great concentration gradient between the outside and the inside of the resin particles, which, in turn, improves the mass transfer in the particle. Nestle and Kimmich (65) investigated the diffusion of copper in alginate gel beads using NMR imaging. They show that the intraparticle diffusion coefficient was concentration-dependent, following a trend derived from the sorption isotherm that controls metal distribution at equilibrium. In the present case correlating the intraparticle diffusion coefficient with the same type of Langmuir-derived curve was not possible; however, the D_e coefficient increased non-linearly with residual concentration. In the case of Zn(II) sorption using the same kind of EIR, Gallardo et al. (43) did not observe a clear trend in the variation of D_e with metal concentration IL loading. For Au(III) binding using Cyphos IL-101 immobilized in alginate capsules, Campos et al. (40) observed a discontinuous trend in the evolution of D_e with metal concentration. Serarols et al. (27) observed an increase of the intraparticle diffusivity of Au(III) using Amberlite XAD-2 impregnated with triisobutyl phosphine sulfide (from $2.1 \times 10^{-10}\,m^2\,min^{-1}$ to $10.7 \times 10^{-10}\,m^2\,min^{-1}$).

Influence of Temperature on Uptake Kinetics

The temperature slightly affected the sorption isotherms as shown on Fig. 6. The temperature may affect the viscosity of the IL in the porous network. Therefore it is, important to check whether the temperature may affect the mass transfer properties of the resin. Figure 9 compares the kinetic profiles at three different temperatures. The curves were very close for the different temperatures. The largest differences were obtained at T: 40°C (313 K), compared to the kinetics at 10°C and 20°C. Actually, the comparison of D_e (in Table 3) shows a very limited variation of the intraparticle diffusion coefficient when varying temperature: D_e did not vary between 20°C and 40°C and was only decreased by less than 25% less at 10°C. The temperature can be considered a non-limiting parameter, at least in the range 10–40°C.

Gold Desorption and EIR Recycling

Metal desorption and resin recycling are key steps in the design and evaluation of sorption systems. In the case of precious metal ions, the recovery of the metals from loaded phases is frequently performed using a complexing agent such as thiourea (in water or acidic solutions) in sorption systems (5,6,8,15,66,67) or solvent extraction systems (25), or EIR (29,40). Preliminary investigations were performed with a single rinsing step (using 0.01 M HCl solution). In this case the sorption efficiency progressively decreased and so also the desorption efficiency. Additionally, at the first step a dark yellow- to coffee-colored precipitate was observed. The precipitate was dissolved in aqua regia and found to contain gold. This loss in sorption and desorption efficiency was attributed to the presence of residual amounts of thiourea that caused partial metal precipitation. This problem was eliminated by increasing the number of rinsing steps (in order to improve thiourea washing between desorption and sorption steps). With the three-rinsing mode, the sorption and desorption efficiencies were maintained at high level (above 99%) for at least five cycles.

CONCLUSION

Gold(III) can be efficiently recovered from HCl solutions using Cyphos IL-101 immobilized on Amberlite XAD-7 resins. Under very acidic conditions (i.e., HCl concentration above 1 M), the resin is chemically modified by partial hydrolysis of acrylic ester groups ($=O\cdot\cdot H^+Cl^-$), and gold is extracted as an anionic chloro-complex ($=O\cdot\cdot H^+AuCl_4^-$) by exchange with chloride ions. The impregnation of the resin with Cyphos IL-101 allows increasing the sorption capacity up to $160\,mg\,Au\,g^{-1}$ through an ion exchange process involving interaction between protonated $R_3R'P^+$ groups and anionic gold chloro-complexes. SEM-EDAX analysis shows that the IL was homogeneously distributed in the EIR and that gold was homogeneously adsorbed in the whole mass of the resin, except at the center. At the center, a greater density of Au is observed, which is attributed to the formation of large aggregates. Additional studies are planned to further investigate this phenomenon. At saturation of the EIR the molar ratio between Au(III) and IL is close to 1:1; this confirms that gold is bound as the chloro-anionic species. Sorption capacity increases with IL loading up to $400\,mg\,IL\,g^{-1}$; above this loading the excess of IL in the porous network may affect the stability of IL in the polymer matrix. Additionally, the comparison of sorption capacities with IL loading (and taking into account the affinity of free resin for gold at high HCl concentration) indicates that a part of the IL did not contribute to metal binding but interacts with the internal surface of the resin. The thermodynamics of the sorption process indicates that the reaction is spontaneous, endothermic, and leads to an increase in randomness during metal binding. Uptake kinetics are controlled by the resistance to intraparticle diffusion. The intraparticle diffusion coefficient varied between $1.8 \times 10^{-11}\,m^2\,min^{-1}$ and $16.6 \times 10^{-11}\,m^2\,min^{-1}$ and is dependent on IL loading, metal concentration, and temperature. Increasing IL loading decreases the intraparticle diffusion coefficient due to a progressive saturation of the porous network by the IL, which in turn limits mass transfer properties. Desorption can be carried out using thiourea solutions in HCl solutions. The resin must be carefully rinsed after the desorption step to remove residual thiourea that causes metal precipitation (inside the porous network) and subsequent decreases in sorption and desorption efficiencies. Under optimized conditions, the sorption

efficiency and desorption efficiencies reached 99% for at least the first five sorption/desorption cycles.

ACKNOWLEDGEMENTS

The authors thank the Franco-Mexican PCP program (Post-graduate Cooperation Program PCP No. 06/05), and the University of Guanajuato (CIAI 2008, 107/08) for financial support. Cytec Company is acknowledged for the gift of Cyphos IL-101 sample.

REFERENCES

1. Brooks, C.S. (1991) *Metal Recovery from Industrial Wastes*; Lewis Publishers: Chelsea, MI.
2. Ertan, E.; Gulfen, M. (2009) Separation of gold(III) ions from copper(II) and zinc(II) ions using thiourea-formaldehyde or urea-formaldehyde chelating resins. *J. Appl. Polym. Sci.*, 111 (6): 2798.
3. Tuzen, M.; Saygi, K.O.; Soylak, M. (2008) Novel solid phase extraction procedure for gold(III) on Dowex M 4195 prior to its flame atomic absorption spectrometric determination. *J. Hazard. Mater.*, 156 (1–3): 591.
4. Senturk, H.B.; Gundogdu, A.; Bulut, V.N.; Duran, C.; Soylak, M.; Elci, L.; Tufekci, M. (2007) Separation and enrichment of gold(III) from environmental samples prior to its flame atomic absorption spectrometric determination. *J. Hazard. Mater.*, 149 (2): 317.
5. Alguacil, F.J.; Adeva, P.; Alonso, M. (2005) Processing of residual gold(III) solutions via ion exchange. *Gold Bull.*, 38 (1): 9.
6. Sanchez, J.M.; Hidalgo, M.; Salvado, V. (2001) The selective adsorption of gold(III) and palladium(II) on new phosphine sulphide-type chelating polymers bearing different spacer arms – Equilibrium and kinetic characterisation. *React. Funct. Polym.*, 46 (3): 283.
7. Sanchez, J.M.; Hidalgo, M.; Valiente, M.; Salvado, V. (2000) New macroporous polymers for the selective adsorption of gold(III) and palladium(II). I. The synthesis, characterization, and effect of spacers on metal adsorption. *J. Polym. Sci., Part A: Polym. Chem.*, 38 (2): 269.
8. Donia, A.M.; Atia, A.A.; Elwakeel, K.Z. (2005) Gold(III) recovery using synthetic chelating resins with amine, thio and amine/mercaptan functionalities. *Sep. Purif. Technol.*, 42 (2): 111.
9. Ly Arrascue, M.; Maldonado Garcia, H.; Horna, O.; Guibal, E. (2003) Gold sorption on chitosan derivatives. *Hydrometallurgy*, 71 (1–2): 191.
10. Donia, A.M.; Atia, A.A.; Elwakeel, K.Z. (2007) Recovery of gold(III) and silver(I) on a chemically modified chitosan with magnetic properties. *Hydrometallurgy*, 87 (3–4): 197.
11. Parajuli, D.; Khunathai, K.; Adhikari, C.R.; Inoue, K.; Ohto, K. (2009) Total recovery of gold, palladium, and platinum using lignophenol derivative. *Min. Eng.*, 22 (13): 1173.
12. Parajuli, D.; Adhikari, C.R.; Kawakita, H.; Yamada, S.; Ohto, K.; Inoue, K. (2009) Chestnut pellicle for the recovery of gold. *Bioresour. Technol.*, 100 (2): 1000.
13. Parajuli, D.; Inoue, K.; Kawakita, H.; Ohto, K.; Harada, H.; Funaoka, M. (2008) Recovery of precious metals using lignophenol compounds. *Min. Eng.*, 21 (1): 61.
14. Parajuli, D.; Kawakita, H.; Inoue, K.; Ohto, K.; Kajiyama, K. (2007) Persimmon peel gel for the selective recovery of gold. *Hydrometallurgy*, 87 (3–4): 133.
15. Fujiwara, K.; Ramesh, A.; Maki, T.; Hasegawa, H.; Ueda, K. (2007) Adsorption of platinum(IV), palladium(II) and gold(III) from aqueous solutions onto L-lysine modified crosslinked chitosan resin. *J. Hazard. Mater.*, 146 (1–2): 39.
16. Alguacil, F.J.; Alonso, M.; Sastre, A.M. (2005) Facilitated supported liquid membrane transport of gold(I) and gold(III) using Cyanex (R) 921. *J. Membr. Sci.*, 252 (1–2): 237.
17. Alguacil, F.J.; Coedo, A.G.; Dorado, M.T.; Padilla, I. (2001) Phosphine oxide mediate transport: modelling of mass transfer in supported liquid membrane transport of gold(III) using Cyanex 923. *Chem. Eng. Sci.*, 56 (10): 3115.
18. de San Miguel, E.R.; Garduno-Garcia, A.V.; Nunez-Gaytan, M.E.; Aguilar, J.C.; de Gyves, J. (2008) Application of an organic-inorganic hybrid membrane for selective gold(III) permeation. *J. Membr. Sci.*, 307 (1): 1.
19. Chowdhury, D.A.; Kamata, S. (1997) Neutral bifunctional phosphonates as reagents for solvent extraction of Au(III): Selective recovery of gold from hydrochloric acid solutions using tetrabutyl 1,3-xylylenediphosphonate. *Solvent Extr. Ion Exch.*, 15 (2): 231.
20. Dominguez, M.; Antico, E.; Beyer, L.; Aguirre, A.; Garcia-Granda, S.; Salvado, V. (2002) Liquid-liquid extraction of palladium(II) and gold(III) with N-benzoyl-N′,N′-diethylthiourea and the synthesis of a palladium benzoylthiourea complex. *Polyhedron*, 21 (14–15): 1429.
21. Duche, S.N.; Mhaske, A.A.; Dhadke, P.M. (2002) Extraction behaviour of gold(III) from bromide media using some neutral organophosphine extractants. *J. Indian Chem. Soc.*, 79 (7): 599.
22. El-Shahawi, M.S.; Bashammakh, A.S.; Bahaffi, S.O. (2007) Chemical speciation and recovery of gold(I, III) from wastewater and silver by liquid-liquid extraction with the ion-pair reagent amiloride mono hydrochloride and AAS determination. *Talanta*, 72 (4): 1494.
23. Guo, J.X.; Sun, X.; Yin, Z.L.; Li, X.M.; Yu, H.Y.; Yang, Y.Z.; Sun, S.X. (2003) Solvent extraction of gold(III) by octadecyldimethylbenzylammonium chloride (ODMBAC) from chloride solution. *J. Radioanal. Nucl. Chem.*, 256 (3): 595.
24. Kolekar, S.S.; Anuse, M.A. (2001) Rapid solvent extraction of gold(III) with high molecular weight amine from organic acid solution. *Gold Bull.*, 34 (2): 50.
25. Narita, H.; Tanaka, M.; Morisaku, K.; Abe, T. (2006) Extraction of gold(III) in hydrochloric acid solution using monoamide compounds. *Hydrometallurgy*, 81 (3–4): 153.
26. Shetkar, P.B.; Gaudh, J.S.; Shinde, V.M. (1997) Extraction of gold(III) with triphenylphosphine sulfide and subsequent spectrophotometric determination. *Sep. Sci. Technol.*, 32 (11): 1937.
27. Serarols, J.; Poch, J.; Llop, M.F.; Villaescusa, I. (1999) Determination of the effective diffusion coefficient for gold(III) on a macroporous resin XAD-2 impregnated with triisobutyl phosphine sulfide. *React. Funct. Polym.*, 41 (1): 27.
28. Villaescusa, I.; Salvado, V.; De Pablo, J.; Valiente, M.; Aguilar, M. (1992) Liquid solid extraction of gold(III) from aqueous chloride solutions by macroporous resins impregnated with triisobutyl phosphine sulfide (Cyanex −471). *React. Polym.*, 17 (1): 69.
29. Villaescusa, I.; Salvadó, V.; de Pablo, J. (1996) Liquid-liquid and solid-liquid extraction of gold by trioctylmethylammonium chloride (TOMAC1) dissolved in toluene and impregnated on amberlite XAD-2 resin. *Hydrometallurgy*, 41 (2–3): 303.
30. Dietz, M.L. (2006) Ionic liquids as extraction solvents : Where do we stand? *Sep. Sci. Technol.*, 41 (10): 2047.
31. Nakashima, K.; Kubota, F.; Maruyama, T.; Goto, M. (2005) Feasibility of ionic liquids as alternative separation media for industrial solvent extraction processes. *Ind. Eng. Chem. Res.*, 44 (12): 4368.
32. Visser, A.E.; Swatloski, R.P.; Reichert, W.M.; Griffin, S.T.; Rogers, R.D. (2000) Traditional extractants in nontraditional solvents: Groups 1 and 2 extraction by crown ethers in room-temperature ionic liquids. *Ind. Eng. Chem. Res.*, 39 (10): 3596.
33. Ciezynska, A.; Regel-Rosocka, M.; Wisniewski, M. (2007) Extraction of palladium(II) ions from chloride solutions with phosphonium ionic liquid Cyphos IL101. *Pol. J. Chem. Technol.*, 9 (2): 99.

34. Regel-Rosocka, M. (2009) Extractive removal of zinc(II) from chloride liquors with phosphonium ionic liquids/toluene mixtures as novel extractants. *Sep. Purif. Technol.*, 66 (1): 19.
35. Marták, J.; Schlosser, Š. (2007) Extraction of lactic acid by phosphonium ionic liquids. *Sep. Purif. Technol.*, 57 (3): 483.
36. Marták, J.; Schlosser, Š.; Vlčková, S. (2008) Pertraction of lactic acid through supported liquid membranes containing phosphonium ionic liquid. *J. Membr. Sci.*, 318 (1–2): 298.
37. Vincent, T.; Parodi, A.; Guibal, E. (2008) Immobilization of Cyphos IL-101 in biopolymer capsules for the synthesis of Pd sorbents. *React. Funct. Polym.*, 68 (7): 1159.
38. Vincent, T.; Parodi, A.; Guibal, E. (2008) Pt recovery using Cyphos IL-101 immobilized in biopolymer capsules. *Sep. Purif. Technol.*, 62 (2): 470.
39. Guibal, E.; Gavilan, K.C.; Bunio, P.; Vincent, T.; Trochimczuk, A. (2008) Cyphos IL 101 (tetradecyl(trihexyl)phosphonium chloride) immobilized in biopolymer capsules for Hg(II) recovery from HCl solutions. *Sep. Sci. Technol.*, 43 (9–10): 2406.
40. Campos, K.; Vincent, T.; Bunio, P.; Trochimczuk, A.; Guibal, E. (2008) Gold recovery from HCl solutions using Cyphos IL-101 (a quaternary phosphonium ionic liquid) immobilized in biopolymer capsules. *Solvent Extr. Ion Exch.*, 26 (5): 570.
41. Campos, K.; Domingo, R.; Vincent, T.; Ruiz, M.; Sastre, A.M.; Guibal, E. (2008) Bismuth recovery from acidic solutions using Cyphos IL-101 immobilized in a composite biopolymer matrix. *Water Res.*, 42 (14): 4019.
42. Vincent, T.; Guibal, E.; Chiarizia, R. (2007) Palladium recovery by reactive precipitation using a Cyanex 301-based stable emulsion. *Sep. Sci. Technol.*, 42 (16): 3517.
43. Gallardo, V.; Navarro, R.; Saucedo, I.; Avila, M.; Guibal, E. (2008) Zinc(II) extraction from hydrochloric acid solutions using amberlite XAD-7 impregnated with Cyphos IL-101 (tetradecyl(trihexyl)phosphonium chloride). *Sep. Sci. Technol.*, 43 (9–10): 2434.
44. Guibal, E.; Vincent, T.; Jouannin, C. (2009) Immobilization of extractants in biopolymer capsules for the synthesis of new resins: a focus on the encapsulation of tetraalkyl phosphonium ionic liquids. *J. Mater. Chem.*, 19 (45): 8515.
45. Guibal, E.; Figuerola Pinol, A.; Ruiz, M.; Vincent, T.; Jouannin, C.; Sastre, A. (2010). Immobilization of Cyphos ionic liquids in alginate capsules for Cd(II) sorption. *Sep. Sci. Technol.*, DOI: 10.1080/01496395.2010.493113
46. Juang, R.-S. (1999) Preparation, properties and sorption behavior of impregnated resins containing acidic organophosphorus extractants. *Proc. Natl. Sci. Counc. ROC(A)*, 23 (3): 353.
47. Hinojosa Reyes, L.; Saucedo Medina, T.I.; Navarro Mendoza, R.; Revilla Vasquez, J.; Avila Rodriguez, M.; Guibal, E. (2001) Extraction of cadmium from phosphoric acid using resins impregnated with organophosphorus extractants. *Ind. Eng. Chem. Res.*, 40 (5): 1422.
48. Navarro, R.; González, M.P.; Saucedo, I.; Avila, M.; Prádanos, P.; Martínez, F.; Martín, A.; Hernández, A. (2008) Effect of an acidic treatment on the chemical and charge properties of a nanofiltration membrane. *J. Membr. Sci.*, 307 (1): 136.
49. Koshima, H. (1986) Adsorption of iron(III), gold(III), gallium(III), thallium(III), and antimony(V) on Amberlite XAD and Chele × 100 resine from hydrochloric acid solution. *Anal. Sci.*, 2 (3): 255.
50. Navarro, R.; Gallardo, V.; Saucedo, I.; Guibal, E. (2009) Extraction of Fe(III) from hydrochloric acid solutions using Amberlite XAD-7 resin impregnated with trioctylphosphine oxide (Cyanex 921). *Hydrometallurgy*, 98 (3–4): 257.
51. Laatikainen, M.; Paatero, A. (2005) Gold recovery from chloride solutions with XAD-7: Competitive adsorption of Fe(III) and Te(IV). *Hydrometallurgy*, 79 (3–4): 154.
52. Baes, C.F.; Mesmer, R.E. (1976) *The Hydrolysis of Cations*; John Wiley & Sons: New York.
53. Arias, A.; Saucedo, I.; Navarro, R.; Gallardo, V.; Martinez, M.; Guibal, E. (2010). Cadmium(II) recovery from hydrochloric acid solutions using Amberlite XAD-7 impregnated with tetraalkyl phosphonium ionic liquid. *Langmuir*, submitted for publication.
54. Avila-Rodriguez, M.; Cholico, D.F.; Gonzalez, M.P.; Navarro, R.; Saucedo, T.I.; (2009) Recovery of Fe(III) from acidic solutions by SLM using Cyphos IL 101 ionic liquid as carrier. In: *Handbook of Membrane Research: Properties, Performance and Applications*, Gorley, S.V., ed.; Nova Science Publishers: New York.
55. Srivastava, V.C.; Mall, I.D.; Mishra, I.M. (2007) Adsorption thermodynamics and isosteric heat of adsorption of toxic metal ions onto bagasse fly ash (BFA) and rice husk ash (RHA). *Chem. Eng. J.*, 132 (1–3): 267.
56. Martinez, M.; Sastre, A.M.; Alguacil, F.J. (1997) Gold extraction equilibrium in the system Cyanex 921-HCl-Au(III). *Hydrometallurgy*, 46 (1–2): 205.
57. Barroso, M.A.; Lopez, F.A.; Sastre, A.M.; Alguacil, F.J. (1997) Study of the extraction of gold(III) in aqueous hydrochloric acid media by the phosphine oxide Cyanex 925. *Hydrometallurgy*, 45 (1–2): 199.
58. Shu, Y.; Li, L.; Zhang, Q.; Wu, H. (2010) Equilibrium, kinetics and thermodynamic studies for sorption of chlorobenzenes on CTMAB modified bentonite and kaolinite. *J. Hazard. Mater.*, 173 (1–3): 47.
59. Guerra, D.L.; Silva, E.M.; Airoldi, C. (2010) Application of modified attapulgites as adsorbents for uranyl uptake from aqueous solution–Thermodynamic approach. *Process Saf. Environ. Prot.*, 88 (1): 53.
60. Tien, C. (1994) *Adsorption Calculations and Modeling*; Butterworth-Heinemann: Newton, MA.
61. Juang, R.-S.; Ju, C.-Y. (1998) Kinetics of sorption of Cu(II)-ethylenediaminetetraacetic acid chelated anions on cross-linked, polyaminated chitosan beads. *Ind. Eng. Chem. Res.*, 37 (8): 3463.
62. Juang, R.-S.; Lin, H.-C. (1995) Metal sorption with extractant-impregnated macroporous resins. 1. Particle diffusion kinetics. *J. Chem. Technol. Biotechnol.*, 62 (2): 132.
63. Juang, R.-S.; Lin, H.-C. (1995) Metal sorption with extractant-impregnated macroporous resins. 2. Chemical reaction and particle diffusion kinetics. *J. Chem. Technol. Biotechnol.*, 62 (2): 141.
64. Crank, J. (1975) *The Mathematics of Diffusion*, 2nd Ed.; Oxford University Press: Oxford, U.K.
65. Nestle, N.; Kimmich, R. (1996) Concentration-dependent diffusion coefficients and sorption isotherms. Application to ion exchange processes as an example. *J. Phys. Chem.*, 100 (30): 12569.
66. Ramesh, A.; Hasegawa, H.; Sugimoto, W.; Maki, T.; Ueda, K. (2008) Adsorption of gold(III), platinum(W) and palladium(II) onto glycine modified crosslinked chitosan resin. Bioresour. *Technol.*, 99 (9): 3801.
67. Iglesias, M.; Antico, E.; Salvado, V. (1999) Recovery of palladium(II) and gold(III) from diluted liquors using the resin duolite GT-73. *Anal. Chim. Acta*, 381 (1): 61.